

Rock properties of the upper-crust in Central Apennines (Italy) derived from high-resolution 3-D tomography

Stephen Monna

Istituto Nazionale di Geofisica e Vulcanologia, Rome, Italy

Luisa Filippi

Dipartimento della Protezione Civile-Ufficio Servizio Sismico Nazionale, Rome, Italy

Laura Beranzoli and Paolo Favali¹

Istituto Nazionale di Geofisica e Vulcanologia, Rome, Italy

Received 17 December 2002; revised 7 March 2003; accepted 13 March 2003; published 11 April 2003.

[1] High-resolution 3-D P and S-wave velocity models of a central sector of the Apennines (Central Italy) are computed by inverting first arrival times from an aftershock sequence (September–December, 1997) following the M_w 5.7 and M_w 6.0 Umbria-Marche earthquakes that occurred on September 26, 1997. The high quality of the data set, especially for the S-wave, allows us to compute 3-D variations in V_p , V_p/V_s and $V_p \cdot V_s$. The anomalies can be interpreted as lateral changes in rock type and fracturing, which control fluid diffusion and variation in pore pressure. This is in agreement with a poro-elastic view that can be inferred from the spatio-temporal evolution of the seismic sequence. **INDEX TERMS:** 5104 Physical Properties of Rocks: Fracture and flow; 5114 Physical Properties of Rocks: Permeability and porosity; 7230 Seismology: Seismicity and seismotectonics; 8180 Tectonophysics: Evolution of the Earth: Tomography. **Citation:** Monna, S., L. Filippi, L. Beranzoli, and P. Favali, Rock properties of the upper-crust in Central Apennines (Italy) derived from high-resolution 3-D tomography, *Geophys. Res. Lett.*, 30(7), 1408, doi:10.1029/2002GL016780, 2003.

1. Introduction

[2] Tomographic interpretations have been used, both with active and passive seismic techniques, to infer differences in physical properties of rocks [e.g., Robertson, 1987; Koch, 1992; Sanders et al., 1995; Lees and Wu, 2000]. This interpretative approach is based on theoretical models, laboratory observations and *in situ* measurements [Tatham, 1982].

[3] Velocity of seismic waves in sedimentary rocks depends mainly on mineral composition; consolidation and cementation of the rock matrix; porosity (total pore and crack volume), pore and crack geometry and their fluid content; effective rock stress (defined as confining pressure minus pore pressure) and temperature [Schön, 1996]. Pore and crack geometry is described by the aspect-ratio parameter α , that is, the ratio of the minimum dimension to the maximum dimension of the crack or pore ($\alpha = 1$ for a

spherical pore; $\alpha \ll 1$ for a flat crack). Presence of very low α cracks (flat cracks, in the range $10^{-3} \div 10^{-2}$), even in a predominantly porous ($\alpha \sim 1$) sedimentary rock, can have a strong effect on the rock's bulk elastic properties [Tatham, 1982; Koch, 1992].

[4] Ambiguities that usually arise analyzing only V_p and V_s , can be resolved by the use of their ratio and product [Lees and Wu, 2000]. For sedimentary rocks V_p/V_s is sensitive to the presence of pore fluids and to concentration of cracks for a given total porosity. Laboratory and borehole measurements have found V_p/V_s to increase with the concentration of fluid saturated cracks (both micro- and macro-cracks) in a condition of low effective stress [Moos and Zoback, 1983]. In particular, this was also verified for fluid saturated carbonates by Robertson [1987], comparing the model of Toksöz et al. [1976] with *in situ* measurements. The other quantity, $V_p \cdot V_s$, is sensitive to variations of porosity in sedimentary rocks [Iverson et al., 1989; Lees and Wu, 2000]. A lower $V_p \cdot V_s$ value implies an increase of porosity.

[5] In this paper we calculate high-resolution 3-D P and S-wave velocity models of a central sector of the Apennines (Central Italy, Umbria-Marche) by inverting first arrival times from an aftershock sequence occurred from September to December 1997. We interpret V_p , V_p/V_s and $V_p \cdot V_s$ anomalies as produced by different rock types having different pore-pressure and fracturing state.

2. Geology and Tectonics

[6] The Umbria region, is characterized by Pliocene active extensional tectonics [Collettini et al., 2000]. These tectonics generated continental basins with a general NNW-SSE trend, bordered either by WSW-dipping or ENE-dipping normal faults striking in the same direction [Bally et al., 1986; Barchi et al., 1998a]. These faults are interpreted as being dissected by minor trans-extensional oblique elements [Cello et al., 1997]. The largest structural feature in the region is the 100-km-long Val Tiberina basin which is controlled by a ENE-dipping master fault (Alto Tiberina fault) [Barchi et al., 1998a]. East of the Val Tiberina basin, the Colfiorito basin is another minor extensional basin, possibly on the hangingwall of the Alto Tiberina fault, directly affected by the 1997 Umbria-Marche seismic sequence. The sequence started with

¹Also at Università degli Studi "G. d'Annunzio," Campus Universitario, Chieti Scalo, Italy.

Table 1. Rock Types in the Study Volume and Average Properties

| Rock | V _p (km/s) | Depth range (km) | Thickness (km) |
|---------|-----------------------|--------------------|----------------|
| MA (CS) | 5.2 ^a | 0 ÷ 3 ^c | 2 ^c |
| CM (CS) | 6.0 ^b | 0 ÷ 3 ^c | 2 ^c |
| EV | 6.1 ^a | 3 ÷ 6 ^c | |

CS = Carbonatic Sequence, MA = *Maiolica* type, CM = *Calcare Massiccio*, EV = Evaporites (Anhydrite). Adapted values from:

^aBarchi *et al.* [1998b].

^bBally *et al.* [1986].

^cBoncio and Lavecchia [2000].

M_w 5.7 and M_w 6.0 earthquakes that were followed by intense swarm (more than 2,500 events) migrating towards SE. The epicentral region occupies a 12 × 40 km² area extending parallel to the Apennines, and the hypocenters were confined within 8 km in depth [Deschamps *et al.*, 2000; Michelini *et al.*, 2000].

[7] The main geologic units in the area are, starting from the surface: Miocene Plio-Pleistocene turbidites, Jurassic-Paleogene carbonatic sequence, Triassic evaporates (anhydrites). Table 1 shows representative members of groups of rocks having similar material properties largely comprised in our study volume, and estimates of their average V_p, depth of maximum concentration and layer thickness in which they predominate.

3. Data and Method

[8] We used P and S-wave arrival times from the Italian National Seismic Network managed by INGV and from digital three-component temporary networks operated by different Italian and French institutions from September 26 to November 3 [Deschamps *et al.*, 2000, Michelini *et al.*, 2000]. From the original data set of 2,538 located events, we selected earthquakes with at least 10 phases (P and/or S) read, gaps smaller than 150 degrees and total RMS residuals smaller than 0.5 s. The final data set used for the inversion consists of 1,125 well-located earthquakes recorded on 39 stations. This resulted in 16,417 P- and 15,598 S-phase first arrival times. The distribution of stations and events allow the investigation of a volume extending about 24 × 40 × 6 km³ (Figure 1a).

Table 2. Best-Fitting 1-D Starting Model^a

| Depth (km) | -2 | 2 | 4 | 6 | 8 |
|-----------------------|-----|-----|-----|-----|-----|
| V _p (km/s) | 4.1 | 5.6 | 6.2 | 6.4 | 6.8 |

^aOrigin of depth scale is at sea level.

[9] Calculation of an accurate 3-D velocity model requires at least a good initial 1-D velocity model. The initial 1-D model used in this study was obtained by inversion of the P-wave data for a best-fit depth-varying 1-D model using the method of Kissling *et al.* [1994, 1995] and 1-D models available from literature [Boncio *et al.*, 1998; Michelini *et al.*, 2000; Alessandrini *et al.*, 2001]. The best-fitting model (Table 2) was then used to relocate the earthquake sequence.

[10] We used the inversion method of Benz *et al.* [1996], which has been applied to understanding seismicity patterns and geology and volcanic structures [Okubo *et al.*, 1997; Villaseñor *et al.*, 1998]. This method uses a finite difference technique [Podvin and Lecomte, 1991] to compute accurate travel times through a complex velocity structure and the efficient least squares QR (LSQR) algorithm [Paige and Saunders, 1982] for simultaneous inversion for the velocity structure and hypocenters. Smoothing constraints are applied to control the degree of model roughness allowed in the inversion. An optimal inversion block size is controlled by the source-receiver geometry (i.e. distance between adjacent stations and the distribution of seismicity) and determined by trial inversions carried out with different block sizes and checkerboard synthetic tests. Trial results determined that the most appropriate inversion cell size is 2 × 2 × 1 km (larger in the horizontal dimension). To ensure accurate calculations of the travel times through the model, we used 1 × 1 × 0.5 km constant velocity cells. The smoothing parameter value was gradually decreased during the iteration process, allowing for a compromise between model stability and minimization of the data misfit.

[11] The final P and S-wave velocity model resulted in a 26% and 20% reduction in the arrival-time RMS, respectively. The initial S-wave velocity model was derived from the initial P-wave model using V_p/V_s = 1.85, calculated from the least square fit between the P and S wave travel time pairs.

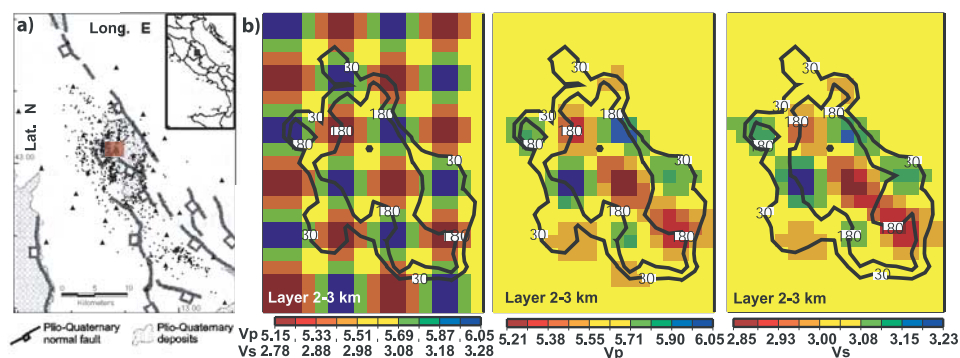


Figure 1. All figures represent the same area. The red square (a) and black dot (b) represent Cofiorito town area. (a) Map of the studied area: Dots represent re-located selected events and triangles the used stations. (Adapted from Boncio and Lavecchia [2000]). (b) Checkerboard test: Input model for the layer 2–3 km is on the left, P- and S-wave output on the right side. Contour lines, also reported on the input image for comparison, represent coverage values for 30 and 180 km cumulated ray path per block (about 10 and 60 rays per block, respectively).

Table 3. Anomaly Volumes With Sign and Peak Value

| Volume | $\delta V_p/V_p$ (%) | $\delta\Psi/\Psi$ (%) | $\delta r/r$ (%) | Depth range (km) |
|--------|----------------------|-----------------------|------------------|------------------|
| A | + (6.0) | + (11) | + (2.8) | 1–5 |
| B | – (3.5) | – (3.5) | 0 | 2–6 |
| C | + (2.0) | + (3.5) | 0 | 3–6 |

[12] Checkerboard resolution tests for both the P- and S-wave dataset show that velocity anomalies larger than about 8 km on a side are well-determined to depth of approximately 6 km (Figure 1b). The test also showed that the significant anomalies discussed in the study are within well-resolved portions of the model. The average value of the reconstructed anomaly contrast is around $\pm 5\%$, a value comparable to the ones found in other tomography studies of the same area [Michelini *et al.*, 2000, Alessandrini *et al.*, 2001]. Furthermore, significant anomalies are within areas that are well sampled (more than 10 rays per block), as evident from the analysis of P- and S-wave ray-path coverage.

4. Results and Interpretation

[13] Map views of percent variations of V_p and percent perturbations of $\Psi = V_p \cdot V_s$ and $r = V_p/V_s$ [Lees and Wu,

2000] of three significant 1-km thick layers are reported in Figure 2. We clearly identify three anomaly volumes within the well covered part of our study area: A) SE of Colfiorito, the most noticeable, where we have positive V_p , r and Ψ anomalies; B) NW of Colfiorito, where we have negative V_p and Ψ anomalies and average values of r ; C) W of Colfiorito, NW-SE direction, where we find positive V_p and Ψ anomalies and average r values (see Table 3 for a schematic description).

[14] Our model interpretation is based on arguments given in the introduction and knowledge of the area's rock types (see Table 1). We propose the following:

[15] A: A volume of stiffer rock with higher crack density, saturated with fluid under low effective stress so cracks remain open, explaining high r values and high Ψ values. Low effective stress is possibly due to higher pore pressure. Volume A could be mainly formed by stiffer, more permeable, high velocity carbonates (e.g., *Calccare Massiccio*). A similar interpretation is given by Nicholson and Simpson [1985] for a layer with analogous characteristics in the New Madrid area (Central U.S.A.), confirmed by a drilling test.

[16] B: Lower V_p , average r , and lower Ψ values imply a softer rock with smaller crack density and greater porosity. B could be a volume where softer, more porous and lower

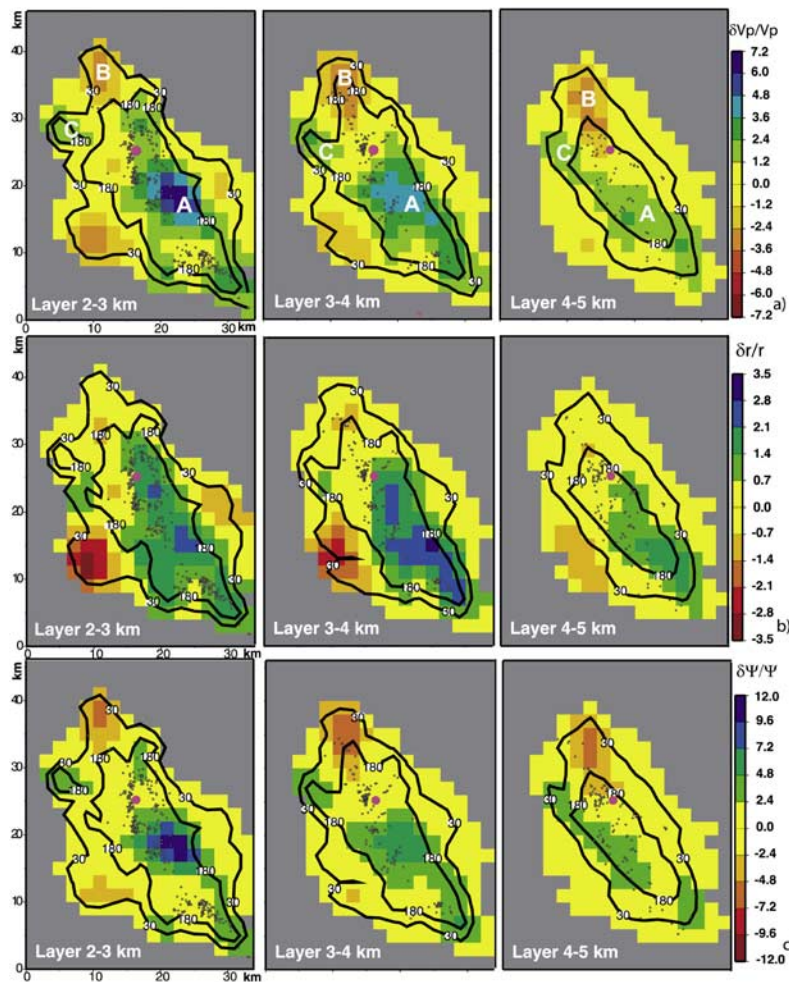


Figure 2. Maps at various depths for $\delta V_p/V_p$ (a), $\delta r/r$ (b) and $\delta\Psi/\Psi$ (c). The colour yellow is associated to the initial 1-D model value for each layer (see Table 2 for initial V_p values). Only seismicity in each layer is depicted. Only blocks covered by at least 1 ray are plotted. The purple dot shows the location of Colfiorito town. Contour lines show coverage for the P-wave (Figure 1a) and S-wave (Figures 1b and 1c).

velocity components of the carbonate sequence are mostly present (e.g., *Maiolica*).

[17] C: Less fractured, low porosity stiffer rock (high Ψ , average r). This could be due to greater presence of high velocity anhydrite (as Triassic evaporite). Interestingly this volume is scarcely affected by seismic activity, implying a more plastic behavior.

[18] Given that the Umbria-Marche aftershock sequence developed for several months, an explanation based on elastic properties only seems unsatisfactory and a poro-elastic approach is preferable. Previous authors have suggested a role of fluid diffusion in the 1997 Umbria-Marche sequence [Cocco et al., 2000; Ripepe et al., 2000] also in agreement with the dilatancy diffusion model of Nur and Booker [1972]. The great majority of aftershock seismic activity evolved in volume A, or at the interface with the other two volumes, where we hypothesize the presence of a stiffer rock, more permeable, fluid saturated, and under high pore pressure. Under such condition we can explain the slow SE migration of the sequence with mobility of fluids in A, gradually increasing pore pressure thus decreasing shear resistance of rock. Presence of evaporite, with low permeability, in the strip-like volume C, could be responsible of a fluid-channeling effect in the NW-SE direction.

[19] A link between the anomaly volumes and structural trends of this area of the Central Apennines will be investigated in a future study.

5. Conclusions

[20] The distribution of a large number of events from the 1997 Umbria-Marche earthquake sequence and a well-distributed local seismic network allowed for the computation of high resolution tomographic images of this part of the Central Apennines. The analysis and comparison of V_p , V_p/V_s and $V_p \cdot V_s$ contributes to our understanding of the geology and rheologic properties of the area. Results show three distinct anomalies, which are interpreted to be produced by changes in porosity, degree of fracturing, and fluid pore pressure. Considering that the study is restricted to depths less than 8 km and that the area is characterized by low heat-flow [Mongelli et al., 1991], temperature is not considered as a controlling factor on velocity variation in the region. Our model agrees with a poro-elastic view of the spatio-temporal evolution of this long-lasting seismic sequence.

[21] **Acknowledgments.** We thank H. M. Benz for his support and advice. B. Alessandrini, C. Doglioni, and F. Frugoni for their helpful suggestions. Many thanks to the colleagues of the former RMS unit of ING, especially R. Azzara and G. Selvaggi, for making the data available. We are also grateful to the colleagues of the Servizio Sistemi di Monitoraggio di DPC-SSN. We thank Roberto Scarpa and an anonymous reviewer for their comments.

References

Alessandrini, B., L. Filippi, and A. Borgia, Upper-crust tomographic structure of the Central Apennines, Italy, from local earthquakes, *Tectonophysics*, 339, 479–494, 2001.

Bally, A. W., L. Burbi, C. Cooper, and R. Ghelardoni, Balanced sections and seismic reflection profiles across the Central Apennines, *Mem. Soc. Geol. It.*, 35, 257–310, 1986.

Barchi, M. R., A. De Feyter, M. B. Magnani, G. Minelli, G. Pialli, and B. M. Sotera, The structural style of the Umbria-Marche fold and thrust belt, *Mem. Soc. Geol. It.*, 52, 557–578, 1998a.

Barchi, M. R., G. Minelli, G. Pialli, and B. M. Sotera, The CROP03 profile: A synthesis of results on deep structures of the Northern Apennines, *Mem. Soc. Geol. It.*, 52, 383–400, 1998b.

Benz, H. M., B. A. Chouet, P. B. Dawson, J. C. Kahr, R. A. Page, and J. A. Hole, Three-dimensional P and S wave velocity structure of Redoubt Volcano, Alaska, *J. Geophys. Res.*, 101, 8111–8128, 1996.

Boncio, P., and G. Lavecchia, A geological model for the Cloriflorio earthquakes (September–October 1997, central Italy), *J. Seismol.*, 4, 345–356, 2000.

Boncio, P., F. Ponziani, F. Brozzetti, M. Barchi, G. Lavecchia, and G. Pialli, Seismicity and extensional tectonics in the Northern Umbria-Marche Apennines, *Mem. Soc. Geol. It.*, 52, 539–555, 1998.

Cello, G., S. Mazzoli, E. Tondi, and E. Turco, Active tectonics in the Central Apennines and possible implications for seismic hazard analysis in peninsular Italy, *Tectonophysics*, 272, 43–68, 1997.

Cocco, M., C. Nostro, and G. Ekstrom, Static stress changes and fault interaction during the 1997 Umbria-Marche earthquake sequence, *J. Seismol.*, 4, 501–516, 2000.

Collettini, C., M. Barchi, C. Pauselli, C. Federico, and G. Pialli, Seismic expression of active extensional faults in northern Umbria (central Italy), *J. Geodyn.*, 29, 309–321, 2000.

Deschamps, A., et al., Spatio-temporal distribution of seismic activity during the Umbria-Marche crisis, 1997, *J. Seismol.*, 4, 377–386, 2000.

Iverson, W. P., B. A. Fahmy, and S. B. Smithson, $V_p \cdot V_s$ from mode-converted P-SV reflections, *Geophysics*, 54, 843–852, 1989.

Kissling, E., W. L. Ellsworth, D. Eberhart-Phillips, and U. Kradolfer, Initial reference models in local earthquake tomography, *J. Geophys. Res.*, 99, 19,635–19,646, 1994.

Kissling, E., U. Kradolfer, and H. Maurer, VELEST user's guide-short introduction, technical report, Inst. of Geophys. and Swiss Seismol. Serv., Eidg. Tech. Hochsch., Zurich, 1995.

Koch, M., Bootstrap inversion for vertical and lateral variations of the S wave structure and the V_p/V_s -ratio from shallow earthquakes in the Rhinegraben seismic zone, Germany, *Tectonophysics*, 210, 91–115, 1992.

Lees, J. M., and H. Wu, Poisson's ratio and porosity at Coso geothermal area, California, *J. Volcanol. Geotherm. Res.*, 95, 157–173, 2000.

Michelini, A., D. Spallarossa, M. Cattaneo, A. Govoni, and A. Montanari, The 1997 Umbria-Marche (Italy) earthquake sequence: Tomographic images obtained from data of the GNDT-SSN temporary network, *J. Seismol.*, 4, 415–433, 1997.

Mongelli, F., G. Zito, B. Della Vedova, G. Pellis, P. Squarci, and L. Taffi, Geothermal regime of Italy and surrounding seas, in *Exploration of the Deep Continental Crust*, edited by V. Ceramak and L. Rybach, pp. 381–394, Springer-Verlag, New York, 1991.

Moos, D., and M. D. Zoback, In situ studies of velocity in fractured crystalline rocks, *J. Geophys. Res.*, 88, 2345–2358, 1983.

Nicholson, C., and D. W. Simpson, Changes in V_p/V_s with depth: Implications for appropriate velocity models, improved earthquake locations, and material properties of the upper crust, *Bull. Seismol. Soc. Am.*, 75, 1105–1123, 1985.

Nur, A., and J. R. Booker, Aftershocks caused by pore fluid flow?, *Science*, 175, 885–887, 1972.

Okubo, P. G., H. M. Benz, and B. A. Chouet, Imaging the crustal magma source beneath Mauna Loa and Kilauea Volcanoes, Hawaii, *Geology*, 25, 867–870, 1997.

Paige, C. C., and M. A. Saunders, LSQR: An algorithm for sparse linear equations and sparse least squares, *Trans. Math. Software*, 8, 43–71, 1982.

Podvin, P., and I. Lecompte, Finite difference computation of travel times in very contrasted velocity models: A massively parallel approach and its associated tools, *Geophys. J. Int.*, 105, 271–284, 1991.

Ripepe, M., D. Piccinini, and L. Chiaraluce, Foreshock sequence of the September 26th, 1997 Umbria-Marche earthquakes, *J. Seismol.*, 4, 387–389, 1997.

Robertson, J. D., Carbonate porosity from S/P traveltimes ratios, *Geophysics*, 52, 1346–1354, 1987.

Sanders, C. O., L. D. Nixon, and E. A. Schwartz, Seismological evidence for magmatic and hydrothermal structure in Long Valley caldera from local earthquake attenuation and velocity tomography, *J. Geophys. Res.*, 100, 8311–8326, 1995.

Schön, J. H., Physical properties of rocks, in *Handbook of Geophysical Exploration Seismic Exploration*, vol. 18, edited by K. Helbig and S. Treitel, Pergamon, New York, 1996.

Tatham, R. H., V_p/V_s and lithology, *Geophysics*, 47, 336–344, 1982.

Toksöz, M. N., C. H. Cheng, and T. Aytekin, Velocities of seismic waves in porous rock, *Geophysics*, 41, 621–645, 1976.

Villaseñor, A., H. M. Benz, L. Filippi, G. De Luca, R. Scarpa, G. Patané, and S. Vinciguerra, Three-dimensional P-wave velocity structure of Mt. Etna, Italy, *Geophys. Res. Lett.*, 25, 1975–1978, 1998.

L. Beranzoli, P. Favali, and S. Monna, Istituto Nazionale di Geofisica e Vulcanologia, Via di Vigna Murata 605, 00143 Roma, Italy. (monna@ingv.it)
L. Filippi, Dipartimento della Protezione Civile-Ufficio Servizio Sismico Nazionale, Via Curtatone 3, 00185 Roma, Italy.